

Topological Protected Dirac Cones in Compressed Bulk Black Phosphorus

Ruixiang Fei, Vy Tran and Li Yang¹

¹*Department of Physics, Washington University in St. Louis, St. Louis, MO 63130, USA*

(Dated:)

Using the $k \cdot p$ theory and first-principles simulations, we report that applying a moderate pressure (> 0.6 GPa) on black phosphorus can diminish its band gap and produce one-dimensional and even two-dimensional (2D) Dirac cones, distinguishing this material for use in novel non-compound topological insulators. Similar to topological insulators, these 2D Dirac cones result from two competing mechanisms: the unique linear band dispersion tends to open a gap via a “pseudo spin-orbit” coupling, while the band symmetry requirements preserve the material’s gapless spectrum. Moreover, these unique Dirac cones are bulk states that do not require time-reversal symmetry, thus they are robust even in the presence of surface or magnetic perturbations. Ultimately, we show that our predictions can be detected by the material’s unusual Landau levels.

PACS numbers:

To date Dirac materials, such as graphene [1, 2], topological insulators (TIs) [3–5] or spin Hall insulators (SHIs) [6, 7], topological crystalline insulators (TCIs) [8, 9] and Weyl semimetals (WSs) [10, 11], have drawn tremendous research interest. Graphene hosts two-dimensional (2D) Dirac fermions [12, 13]; TIs are materials with a bulk energy gap but possess gapless 2D (1D) Dirac surface states that are protected by time-reversal symmetry [14, 15]; TCIs exhibit metallic surface states protected by the mirror symmetry of the crystal [9]; WSs, which are protected by crystal symmetries, exhibit energy overlaps that occur only at a set of isolated points in momentum space where the linearly dispersed bands cross at the Fermi level [10]. The impact and implications of these materials are difficult to overstate. The discovery of the anomalous Hall effect [16, 17], the fractional Hall effect [18], chiral anomaly [19, 20], and Majorana fermions [21, 22], to name a few, have inspired enormous efforts in search for new Dirac materials.

Recently a new type of 2D semiconductor, few-layer black phosphorus (BP) (phosphorene), has been fabricated [23–25]. It exhibits promising carrier mobilities and unique anisotropic transport, optical, and thermal properties [23–29]. In particular, few-layer BP possesses a unique band structure, whose dispersion is nearly linear along the armchair direction but parabolic along other directions [30, 31]. An obvious idea follows from this unique structure: if one can significantly reduce the band gap or even achieve the band inversion, novel features may result, e.g., the formation of Dirac cones. However, the band gap of monolayer and few-layer BP is significant (up to 2.2 eV) [26, 29, 32], making it impractical to close. Alternatively, bulk black phosphorus has a much smaller band gap, only around 300 meV [26, 33], which is more tractable.

In this work, we show that the $k \cdot p$ Hamiltonian of bulk BP can be written as the free-electron-gas Hamiltonian with off-diagonal terms for describing interband interactions, which are of the same form as the Rashba and Dresselhaus spin-orbit coupling (SOC). Thus we call this off-diagonal interaction the “pseudo spin-orbit” cou-

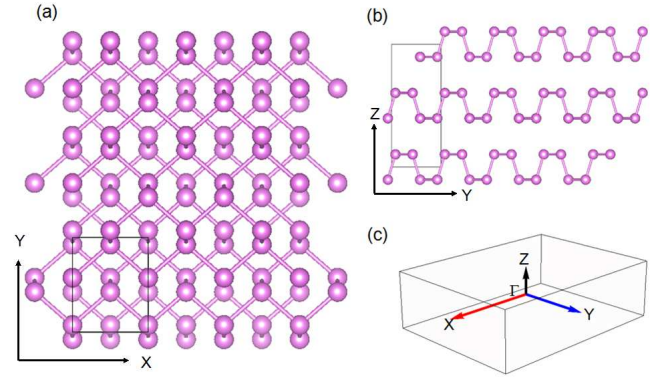


FIG. 1: (Color online) (a) Top view of the atomic structure of bulk BP. The unit cell and lattice vectors are marked. The zigzag and armchair directions are illustrated as well. (b) Side view of BP. (c) The first BZ.

pling (PSOC). If the band gap is diminished and the band inversion is realized, PSOC tends to open a gap in the energy spectrum. However, similar to TIs, the band symmetry requires band connections. Competition between PSOC and band symmetry causes the Fermi surface to undergo a topological transition from a sphere to a ring of 2D Dirac cones. Using first-principles simulations, we show that pressure can be an efficient tool to produce these 2D Dirac cones and even 1D Dirac cones, while also tuning the characteristic Fermi velocity. Interestingly, because our predicted Dirac cone feature in compressed BP does not require the time reversal symmetry, it is not destroyed by magnetic fields. Thus we provide a means for detecting this unique electronic structure by demonstrating the unusual energy scaling law exhibited by Landau levels.

The atomic structure of bulk BP is plotted in Figures 1 (a) and (b). Here we use a simple orthorhombic conventional unit cell, which is twice the size of the primitive cell. The corresponding first Brillouin Zone (BZ) is shown in Figure 1 (c). The double-cell procedure sim-

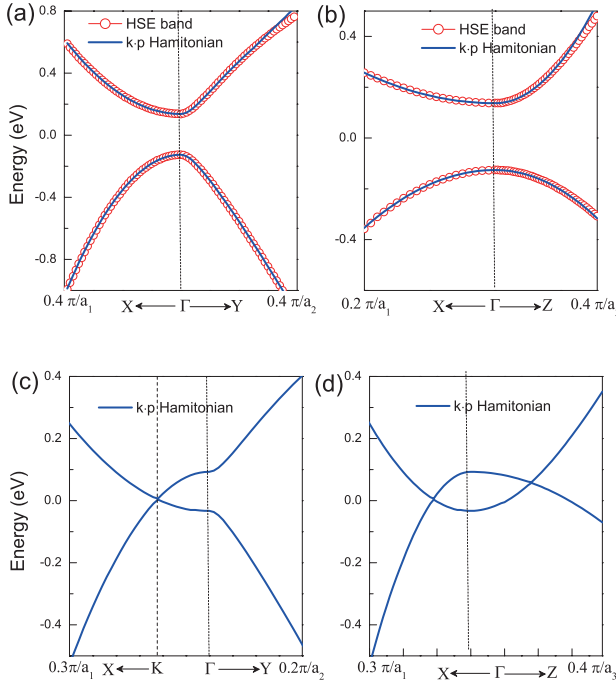


FIG. 2: (Color online) (a) and (b) are the band structures of intrinsic BP. The red dots are from the HSE06 simulation and the blue line is from the $k \cdot p$ calculations. (c) and (d) are the band structures calculated from the $k \cdot p$ calculations under the band-inversion condition. The Fermi level is set to be zero.

ply folds the first BZ and does not affect any essential physics; this is convenient for presenting the topology of the Dirac cones. The bulk BP atomic structures is fully relaxed according to the forces and stresses calculated using density functional theory (DFT) with the Perdew, Burke and Ernzerhof (PBE) functional associated with van der Waals corrections [34, 35]. Because DFT is known to underestimate the band gap, we use a hybrid functional theory (HFT), HSE06 [36, 37], to calculate electronic band structures, which is in good agreement with the GW calculations and experimental measurements [26, 33] of bulk BP.

We begin with the widely used $k \cdot p$ model to capture the essential BP's electronic structure. The D_{2h} point group invariance allows us to describe BP using a two-band model similar to the one used for monolayer BP [38, 39]. Thus the low-energy effective Hamiltonian is given by

$$H = \begin{pmatrix} E_c + \alpha k_x^2 + \beta k_y^2 + \gamma k_z^2 & v_f k_y \\ v_f k_y & E_v - \lambda k_x^2 - \mu k_y^2 - \nu k_z^2 \end{pmatrix} \quad (1)$$

where k_x , k_y , and k_z are components of the crystal momentum along the x , y , and z directions, respectively. The conduction band and the valence band energies, $E_c = 0.15$ eV and $E_v = -0.15$ eV, are set to fit the bulk band gap (300 meV). α , β , γ , λ , μ , and ν are fitted

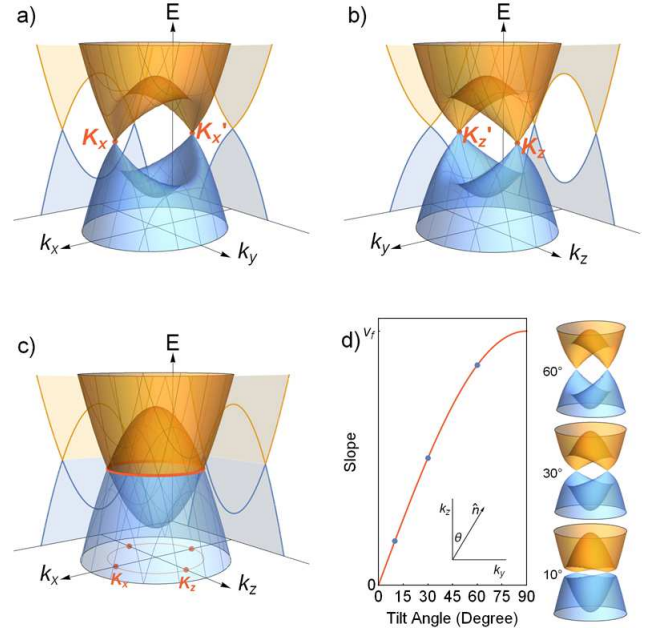


FIG. 3: (Color online) The 3D band structures of BP of the X-Y plane (a), the Y-Z plane (b), and the X-Z plane (c). The band overlap in (c) forms a ring structure. (d) The evolution of the band structure from the X-Z plane to the X-Y plane via changing of the tilted angle.

parameters that describe the band edge curvature, and v_f is the Fermi velocity of the nearly linear band dispersion along the armchair (y) direction. By appropriately choosing these parameters, as shown in Figures 2 (a) and (b), the $k \cdot p$ result nearly perfectly matches that of the first-principles HSE06 calculations of intrinsic BP.

The special characteristics of Eq. 1 are the off-diagonal terms of the effective Hamiltonian, which produce the unique linear dispersion along the armchair (y) direction, as shown in Figure 2 (a). In fact, This off-diagonal interaction can be split into two terms

$$H_{off} = H_{DSOC} + H_{RSOC} \\ = 1/2 v_f (k_x \sigma_y + k_y \sigma_x) - 1/2 v_f (k_x \sigma_y - k_y \sigma_x), \quad (2)$$

where σ_x and σ_y are Pauli matrices. Interestingly, these two terms (H_{DSOC} and H_{RSOC}) have the forms of the Dresselhaus and Rashba SOC [40], respectively. Realistically, Dresselhaus and Rashba SOC cannot exist in intrinsic bulk BP, because its lattice structure possesses the inversion symmetry. Hence we call these interactions PSOC. Because of their similar formalisms, we expect equivalent "SOC effects" to appear in bulk BP. In particular, considering the dramatic effect of SOC in TIs, it is natural to expect that diminishing or inverting the band gap in bulk BP will produce novel electronic characteristics.

It is easy to mimic the band inversion in the $k \cdot p$ model; one simply assigns the valence band edge energy E_v a higher value than the conduction band edge energy

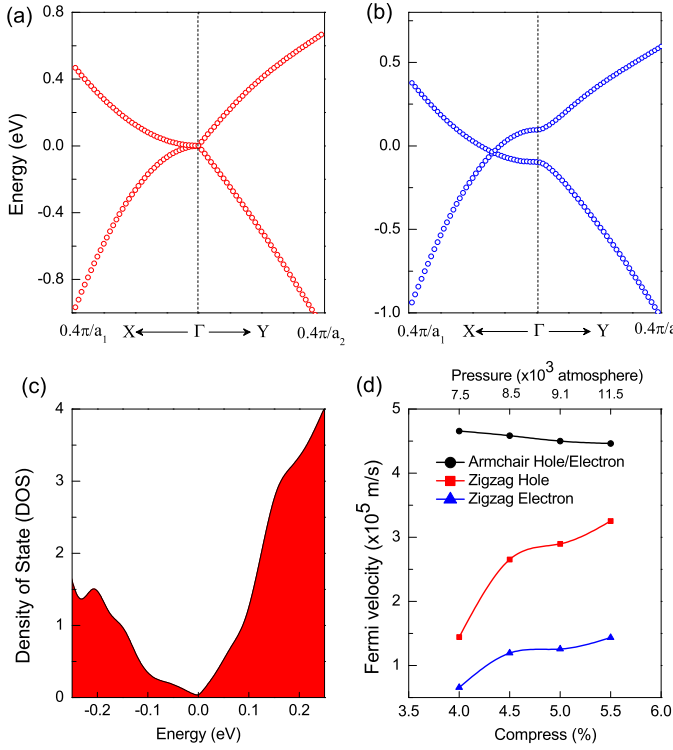


FIG. 4: (Color online)(a) The HSE06-calculated band structure of BP under the critical pressure (0.6 GPa). (b) The HSE06-calculated band structure of BP under the 0.9 GPa pressure. (c) The Anisotropic fermi velocity of electrons and holes of 2D Dirac cones varied with the pressure.

E_c in Eq. 1. Surprisingly, instead of producing simple band overlaps, we observe an unusual topological transition at the Fermi surface. In Figures 2 (c) and (d), the band crossing at the Γ point is opened by the PSOC, while the band crossing is preserved at the K point in the $\Gamma-X$ direction. As a result, 2D graphene-like Dirac cones are formed and the Schematic 3D plots of the electronic structure are presented in Figures 3 (a), (b), and (c) for three specific cutting planes, X-Y, Y-Z and X-Z, respectively. The linear band dispersions and Dirac cones are observed in both X-Y and Y-Z planes and a ring-like band crossing occurs in the X-Z plane. Actually, we can regard the Dirac cones observed in Figure 3 (a) and (b) are those points marked in the ring structures of Figure 3 (c). In this sense, any point on the ring of Figure 3 (c) corresponds to a Dirac cone in other 2D planes. In Figure 3 (d), we show that this ring-like band crossing continuously evolves to a pair of Dirac cones by varying the tilting angles from the X-Z plane to the Y-Z plane. In other words, the set of tilting angles that do not exhibit these Dirac cones is of measure zero, and thus our findings are robust.

The mechanisms responsible for forming the ring of Dirac cones are similar to those in TIs, but there are some crucial differences. First, similar to the band inversion and gap-opening that occurs in TIs due to SOC interac-

tions, the gap-opening at the Γ point of Figure 2 (c) from the PSOC of states residing on the linear band along the $\Gamma-Y$ direction. Second, the gap of BP is not completely opened; the valence and conduction bands still touch at the K point (Figure 2 (c)) or by the ring (Figure 3 (c)). This gapless feature is guaranteed by a symmetry constraint based on two facts: the bottom conduction band is formed by what was originally top valence band prior to the band inversion; the parity symmetries of the top of the valence band and the bottom of the conduction band are inverse to each other, which is evidenced by the bright dipole optical transitions [26]. Therefore, as shown in Figures 2 (c) and 3 (c), contact between the conduction and valence band is required in order to provide a continuous symmetry evolution. This mechanism is similar to the one responsible for forming gapless surface states in TIs [41]. However, there are no surface states in our calculated bulk BP, thus it is the bulk valence and conduction bands that must touch. As a result, these two factors force the formation Dirac cones. Moreover, as proposed by a recent work [42], further breaking the inversion symmetry and including the spin-orbit coupling in few-layer BP will open the bulk band gap and produce surface topological states. Finally, another special characteristic of these bulk Dirac cone states in BP is that they are robust even in the face of broken time reversal symmetry. Therefore, these Dirac cones can uniquely be observed in experiments that employ magnetic fields and are potentially useful for magnetic devices.

Following the above analysis of the $k \cdot p$ model and beyond 2D Dirac cones, 3D Weyl points could be achieved if an extra direction, such as the x or z , also exhibits the off-diagonal linear interband interaction (PSOC) term. Therefore, one may search for Ws by looking for realizing the band inversion of the materials that exhibit nearly linear dispersions along two orthogonal directions.

Beyond the $k \cdot p$ model, an obvious question is how one can practically reduce the band gap or achieve band inversion in BP. Towards this end, we turn to the first-principles simulations for quantitative answers. Our HSE06 calculations show that applying an external pressure along the y (armchair) or x (zigzag) direction produces promising effects. Note that, BP is much softer along the y (armchair) direction because of its anisotropic atomic structure [43]. We find that applying a pressure of 0.75 GPa can shrink the lattice constant along the y direction by 4% but only by 1% and 2% for the x and z directions, respectively. Therefore, we will consider the changes made by applying pressure along the y direction because it can change the atomic structure and corresponding electronic structure more significantly via a relatively small pressure.

First, as shown in Figure 4 (a), an applied critical pressure (0.6 GPa) diminishes the band gap and a 1D Dirac cone is produced along the $\Gamma-X$ direction. This pressure is well within the capability of current high-pressure experiments [44, 45].

Second, larger pressures create a band inversion. Ex-

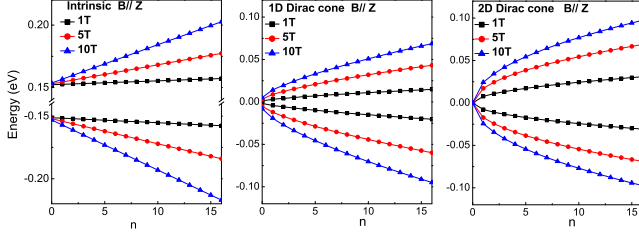


FIG. 5: (Color online) (a) The energy spectrum of Landau levels (index n) of intrinsic BP with magnetic field; (b) that under the critical pressure (0.6 GPa), in which the 1D Dirac cone is formed; (c) That under the pressure of 0.9 GPa, in which 2D Dirac cones are formed.

citingly, similar to the $k \cdot p$ theory predictions, a pressure of 0.9 GPa yields a band crossing at the Γ point and a pair of 2D Dirac cones are formed, as shown in Figure 4 (b). The corresponding density of states (DOS) is shown in Figure 4 (c). We can clearly see that a linear DOS in the low-energy regime, which is similar to graphene. From these first-principles results, we also find that that the Fermi velocities of compressed BP is smaller than that of graphene and that these generated Dirac cones are highly anisotropic in momentum space. Obviously, the Fermi velocities must be anisotropic as well and can be efficiently tuned by varying the applied pressure, as concluded in Figure 4 (d).

We propose that the evolution of the electronic structure from conventional semiconductors to one possessing 1D Dirac cones and 2D Dirac cones can be observed by measuring the energy spectrum of Landau levels; this methodology is widely used for identifying Dirac band structures [2]. For example, considering the X-Y plane, before reaching the critical point for closing the band gap, the energy spectrum of the Landau levels is that of a typical semiconductor, i.e., it is linear with the level index, as shown in Figure 5 (a). Here the spectrum is given by

$$\begin{aligned} E &= E_c + (n + 1/2)\hbar\omega_c \\ E &= E_v - (n + 1/2)\hbar\omega_v, \end{aligned} \quad (3)$$

where the cyclotron frequencies of electrons and holes are $\omega_c = eB/\sqrt{m_{cx}m_{cy}}$ and $\omega_v = eB/\sqrt{m_{vx}m_{vy}}$. m_{cx} , m_{cy} , m_{vx} and m_{vy} are effective mass of electrons and holes along the X and Y directions, respectively. Importantly,

there is no zero-energy solution for this case.

At the critical pressure, a perfectly 1D linear band dispersion along the $\Gamma - Y$ direction simplifies Eq. 1 by setting the parabolic term β and μ to be zero. The effective Hamiltonian with the magnetic field introduced by the Landau gauge $\vec{A} = (-By, 0, 0)$ is

$$\begin{aligned} \frac{1}{2m_c}(\hbar k_x - eBy)^2\phi_A - i\hbar v_f \frac{d}{dy}\phi_B &= E\phi_A, \\ -\frac{1}{2m_v}(\hbar k_x - eBy)^2\phi_B - i\hbar v_f \frac{d}{dy}\phi_A &= E\phi_B, \end{aligned} \quad (4)$$

where $v_f = 3.5 \times 10^5 \text{ m/s}$ is the Fermi velocity of the 1D dirac cone obtained from HSE06 simulations. The corresponding energy spectrum of Landau Levels in magnetic field is presented in Figure 5 (b), which is deviated from the linear relation of Figure 5 (a). Finally, for higher pressures that form 2D Dirac cones, the Landau levels follows the well-known square-root dependence [2, 12], $E_n \propto \sqrt{n}$, and exhibits a unique zero-energy solution, as shown in Figure 5 (c).

In conclusion, we predict that applying a moderate pressure (> 0.6 GPa) on bulk BP can dramatically reshape its band structure. Its band gape will close and band inversion will induce a topological transition of the Fermi surface via the so-called PSOC interaction. Under different pressures, the band dispersions of bulk BP will evolve from that of a semiconductor with a parabolic band dispersions to a semimetal with 1D or 2D Dirac cones that exhibit tunable anisotropic Fermi velocities. Compressed BP thus may be a TI that uniquely integrates both massless Dirac Fermions and massive classical carriers within one material. Furthermore, these bulk Dirac-cone states and robust even under broken time reversal symmetry. Therefore, these unique electronic structures can be identified by Landau levels and we have provided the corresponding energy spectra.

We acknowledge fruitful discussions with Li Chen, Zohar Nussinov and Ryan Soklaski. This work is supported by the National Science Foundation Grant No. DMR-1207141. The computational resources have been provided by the Lonestar and Stampede of Teragrid at the Texas Advanced Computing Center (TACC) and the Edison cluster of the National Energy Research Scientific Computing Center (NERSC). The first-principles calculation is performed with the Vienna ab initio simulation package (VASP) [46].

-
- [1] K. S. Novoselov, A. K. Geim, S. V. Morozov, D. Jiang, M. I. Katsnelson, I. V. Grigorieva, S. V. Dubonos, and A. A. Firsov. Nature **438**, 197-200 (2005).
 [2] Y. Zhang, Y. W. Tan, H. L. Stormer, and Philip Kim. Nature **438**, 201-204 (2005).
 [3] Y. L. Chen, J. G. Analytis, J.-H. Chu, Z. K. Liu, S.-K. Mo, X. L. Qi, H. J. Zhang, D. H. Lu, X. Dai, Z. Fang, S. C. Zhang, I. R. Fisher, Z. Hussain, and Z.-X. Shen.

Science **325**, 178-181(2009).

- [4] D. Hsieh, Y. Xia, D. Qian, L. Wray, J. H. Dil, F. Meier, J. Osterwalder, L. Patthey, J. G. Checkelsky, N. P. Ong, A. V. Fedorov, H. Lin, A. Bansil, D. Grauer, Y. S. Hor, R. J. Cava, and M. Z. Hasan. Nature **460**, 1101-1105 (2009).
 [5] L. Fu, C. L. Kane, and E. J. Mele. Phys. Rev. Lett. **98**, 106803(2007).

- [6] S. Murakami, N. Nagaosa, and S. C. Zhang. Phys. Rev. Lett. **93**, 156804 (2004).
- [7] M. Knig, S. Wiedmann, C. Brne, A. Roth, H. Buhmann, L. W. Molenkamp, X. L. Qi, and S. C. Zhang. Science **318** 766-770 (2007).
- [8] L. Fu. Phys. Rev. Lett. **106**, 106802(2011).
- [9] Y. Tanaka, Z. Ren, T. Sato, K. Nakayama, S. Souma, T. Takahashi, K. Segawa, and Yoichi Ando. Nat. Phys. **8**, 800-803 (2012).
- [10] S. M. Young, S. Zaheer, J. C. Y. Teo, C. L. Kane, E. J. Mele, and A. M. Rappe. Phys. Rev. Lett. **108** 140405(2012).
- [11] Z. K. Liu, B. Zhou, Y. Zhang, Z. J. Wang, H. M. Weng, D. Prabhakaran, S.-K. Mo, Z. X. Shen, Z. Fang, X. Dai, Z. Hussain, and Y. L. Chen. Science **343**, 864-867(2014).
- [12] A. H. Castro Neto, F. Guinea, N. M. R. Peres, K. S. Novoselov, and A. K. Geim. Reviews of Modern Physics **81**, 109 (2009).
- [13] S. Das Sarma, Shaffique Adam, E. H. Hwang, and Enrico Rossi. Reviews of Modern Physics **83**, 407(2011).
- [14] M. Z. Hasan, and C. L. Kane, Reviews of Modern Physics **82**, 3045(2010).
- [15] X. L. Qi, and S. C. Zhang, Reviews of Modern Physics **83**, 1057(2011).
- [16] C. Z. Chang, J. Zhang, X. Feng, J. Shen, Z. Zhang, M. Guo, K. Li, Y. Ou, P. Wei, L. L. Wang, Z. Q. Ji, Y. Feng, S. Ji, X. Chen, J. Jia, X. Dai, Z. Fang, S. C. Zhang, K. He, Y. Wang, L. Lu, X. Ma, and Q. K. Xue, Science **340**, 167-170(2013).
- [17] W. K. Tse, Z. Qiao, Y. Yao, A. H. MacDonald, and Qian Niu. Phys. Rev. B. **83**, 155447(2011) .
- [18] X. Du, I. Skachko, F. Duerr, A. Luican, and E. Y. Andrei. Nature **462**, 192-195(2009).
- [19] A. A. Burkov. Phys. Rev. Lett. **113**, 247203(2014).
- [20] A. A. Zyuzin, and A. A. Burkov. Phys. Rev. Lett. **86**, 115133(2012).
- [21] L. Fu, and C. L. Kane. Phys. Rev. Lett. **100**, 096407(2008).
- [22] A. R. Akhmerov, J. Nilsson, and C. W. J. Beenakker. Phys. Rev. Lett. **102** 216404(2009).
- [23] L. Li, Y. Yu, G. Ye, Q. Ge, X. Ou, H. Wu, D. Feng, X. Chen, and Y. Zhang. Nature nanotechnology **9**, 372 (2014).
- [24] H. Liu , A. T. Neal , Z. Zhu , Z. Luo , X. Xu , D. Tomnek, and P. D. Ye , ACS Nano **8**, 4033 (2014).
- [25] F. Xia, H. Wang, and Y. Jia. Nat. Commun. **5**, 5458(2014).
- [26] V. Tran, R. Soklaski, Y. Liang, and L. Yang. Phys. Rev. B **89**, 235319 (2014).
- [27] Ruixiang Fei, and L. Yang. Nano Lett. **14**, 2884 (2014).
- [28] Ruixiang Fei, A. Faghaninia, R. Soklaski, J. Yan, C. Lo, and Li Yang. Nano Lett. **14**, 63936399 (2014).
- [29] X. Wang, A. M. Jones, K. L. Seyler, V. Tran, Y. Jia, H. Zhao, H. Wang, L. Yang, X. Xu, and F. Xia. arXiv preprint, arXiv:1411.1695 (2014).
- [30] Vy Tran and Li Yang, Phys. Rev. B **89**, 245407 (2014).
- [31] A. S. Rodin, A. Carvalho, and A. H. Castro Neto. Phys. Rev. Lett. **112**, 176801 (2014).
- [32] Liangbo Liang, Jun Wang, Wenzhi Lin, Bobby G. Sumpter, Vincent Meunier, and Minghu Pan, Nano Lett. **14**, 6400 (2014).
- [33] Robert W. Keyes, Phys. Rev. **92**, 580 (1953)
- [34] J. P. Perdew, K. Burke, and M. Ernzerhof. Phys. Rev. Lett. **77**, 3865(1996).
- [35] S. Grimme. J. Chem. Phys. **25**, 1463-1473(2004).
- [36] J. Heyd, G. E. Scuseria, and M. Ernzerhof. J. Chem. Phys. **118**, 8207-8215(2003).
- [37] J. Heyd, G. E. Scuseria, and M. Ernzerhof. J. Chem. Phys. **124**, 219906(2006).
- [38] X. Y. Zhou, R. Zhang, J. P. Sun, Y. L. Zou, D. Zhang, W. K. Lou, F. Cheng, G. H. Zhou, F. Zhai, and K. Chang. arXiv preprint arXiv:1411.4275(2014).
- [39] M. Ezawa. New Journal of Physics **16**, 115004(2014).
- [40] I. utic, J. Fabian, and S. D. Sarma. Reviews of Modern Physics **76**, 323(2004).
- [41] H. Zhang, C. X. Liu, X. L. Qi, X. Dai, Z. Fang, and S. C. Zhang. Nat. Phys. **5**, 438-442 (2009).
- [42] Q. Liu, X. Zhang, L. B. Abdalla, A. Fazzio, and A. Zunger. arXiv preprint arXiv:1411.3932(2014).
- [43] Q. Wei, X. Peng. Appl. Phys. Lett. **104**, 251915(2014).
- [44] Y. Katayama, T. Mizutani, W. Utsumi, O. Shimomura, M. Yamakata, and K. Funakoshi. Nature, **403**, 170-173(2000).
- [45] G. Monaco, S. Falconi, W. A. Crichton, and M. Mezouar. Phys. Rev. Lett. **90**, 255701(2003).
- [46] G. Kresse, and J. Furthmiller. Phys. Rev. B. **54**, 11169(1996).